BHPA-symposium 2022

Scientific Committee

Milan Tomsej (chair), CHU Charleroi

Alain Seret, Université de Liège

Caro Franck, Universitair Ziekenhuis Antwerpen

Damien Dumont, UCLouvain

Kristof Baete, KU Leuven

Lara Struelens, SCK-CEN

Federica Zanca, Palindromo

Koen Tournel, Jessa Ziekenhuis

Nico Buls, UZ Brussel

Gert Van Gompel, UZ Brussel

Thierry Gevaert, UZ Brussel

Scientific Session

Topic: Nuclear Medicine

Chair: Kristof Baete (KU Leuven)

Saturday 30/04/2022 10h40-11h55

Room 11 - 22

Feasibility of lesion dosimetry assuming constant pharmacokinetics over cycles in patients treated with ^{177}Lu-DOTATATE

R. Danieli[1,2], G. Marin[1,] M. Mileva[1], B. Vanderlinden[1], I. Karfis[1], P. Flamen[1], H. Levillain[1]

[1]*Institute Jules Bordet, Belgium*

[2]*Università degli Studi di Pavia, Italy*

KEY WORDS – Add 5 keywords

Introduction

Dosimetry-driven treatment planning in ^{177}Lu-Peptide Receptor Radionuclide Therapy (PRRT) is one of the major challenges in the framework of personalized medicine, with the ultimate goal of improving the clinical outcome of the patients. Invidualised dosimetry requires Multi-Time Point (TP) imaging after each cycle, which is resource consuming for the clinic and burdensome for the patients. The implementation of dosimetry protocols using a reduced number of TPs is therefore essential [1]-[4]. This study aims to evaluate the accuracy of two simplified protocols for lesion dosimetry in patients treated with ^{177}Lu-DOTATATE.

Materials and methods

26 patients with advanced gastroenteropancreatic neuroendocrine neoplasms who received at least 4 cycles of ^{177}Lu-DOTATATE were included. For each patient and cycle, two SPECT/CTs were acquired at 24 and 168 hours post-injection. 56 lesions were segmented on the ^{68}Ga-DOTATATE PET/CT performed 1-3 weeks prior to each ^{177}Lu-DOTATATE cycle using the PETEdge tool of the MIM 6.9 software. The same lesions were segmented on the ^{177}Lu-DOTATATE SPECT/CT using a region-growing tool in order to reach the same volume as the one obtained on ^{68}Ga-DOTATATE PET/CT images. The quantified activity, previously corrected for the partial volume effect, was time-integrated using a mono-exponential fit. Time-Integrated Activity was then converted into absorbed dose (AD) using the OLINDA\EXM 1.1 sphere model.

After performing a preliminary statistical analysis of the variability of the AD per injected activity (AD/IA) and effective half-life (Teff) over treatment cycles, two simplified protocols were selected:

- Protocol A: 2TP dosimetry in C1 and C3 and no imaging in C2 and C4 (i.e. assuming the same AD per injected activity as in the preceding cycle)

- Protocol B: 2TP dosimetry in C1 and a 1TP dosimetry (imaging at 24 h post injection) in subsequent cycles (i.e. assuming the same pharmacokinetics in subsequent cycles)

The one-way ANOVA analysis was used to compare the cumulative AD obtained with Protocol A and B to the reference. The % differences between the cumulative AD and the AD after C2, C3 and C4 were also assessed.

Results

According to the one-way ANOVA analysis, the AD/IA in C1 presented a statistically significant difference from the AD/IA in C3 ($p \leq 0.05$) and C4 ($p \leq 0.001$). Since no statistically significant difference was found for the AD/IA in the other cycles and for the Teff, the choice of Protocol A and Protocol B as possible candidates for a reliable simplified dosimetry is justified.

According to the reference protocol, lesions received a mean cumulative AD of 108 Gy (SD = 52 Gy). Protocol A and Protocol B, instead, provided a mean cumulative AD of 114 Gy (SD = 58 Gy) and 108 Gy (SD = 52 Gy), respectively.

The one-way ANOVA analysis showed a statistically significant difference between Protocol A and the reference ($p \leq 0.0001$). No statistically significant difference was found comparing Protocol B to the reference (Figure 1).

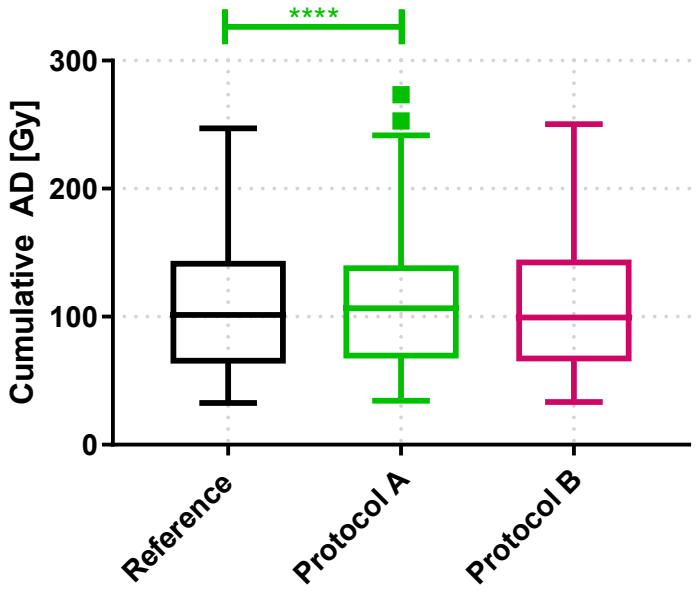

Figure 1: Box-and-whisker plot of the cumulative AD calculated using the reference protocol, Protocol A and Protocol B.

Descriptive statistics of the % differences between the AD calculated with Protocol A, Protocol B and the reference are reported in Table 1.

	Protocol A	Protocol B
Cumulative AD	5% [-16%, -0%, 13%, 25%]	1% [-15%, -4%, 5%, 14%]
AD at C2	15% [-47%, -5%, 39%, 102%]	2% [-27%, -7%, 7%, 16%]
AD at C3	0%	-1% [-17%, -5%, 8%, 26%]
AD at C4	2% [-54%, -10%, 24%, 69%]	4% [-26%, -5%, 11%, 29%]

Table 1: % differences between the AD calculated with Protocol A and Protocol B with respect to the reference. Data are reported as median [min, Q1, Q3, max], outliers excluded.

Conclusion

Our preliminary analysis suggested two interesting options for lesion simplified dosimetry in patients treated with ^{177}Lu-DOTATATE: performing a full dosimetry only in C1 and C3 and assuming a constant Teff over cycles. The comparison between the AD calculated according to these two protocols and the reference showed that the latter provides more accurate results. The introduction of this approach into the clinical routine would significantly reduce the number of required image acquisitions.

References

[1] Chicheportiche, A., Ben-Haim, S., Grozinsky-Glasberg, S. et al. Dosimetry after peptide receptor radionuclide therapy: impact of reduced number of post-treatment studies on absorbed dose

calculation and on patient management. EJNMMI Phys 7, 5 (2020). https://doi.org/10.1186/s40658-020-0273-8

[2] Del Prete, M., Arsenault, F., Saighi, N. et al. Accuracy and reproducibility of simplified QSPECT dosimetry for personalized 177Lu-octreotate PRRT. EJNMMI Phys 5, 25 (2018). https://doi.org/10.1186/s40658-018-0224-9

[3] Freedman, N., Sandström, M., Kuten, J. et al. Personalized radiation dosimetry for PRRT—how many scans are really required?. EJNMMI Phys 7, 26 (2020). https://doi.org/10.1186/s40658-020-00293-z

[4] Hänscheid, H., Lapa, C., Buck, AK. et al. Dose Mapping After Endoradiotherapy with 177Lu-DOTATATE/DOTATOC by a Single Measurement After 4 Days. J Nucl Med. 2018;59(1):75-81. doi:10.2967/jnumed.117.193706

FANC PET transverse uniformity protocol: adaptable to SPECT ?

A. SERET[1], T. CARLIER[2]
[1]*University of Liège, Belgium*
[2]*CHU Nantes, France*

ABSTRACT – This simulation study shows the possibility for SPECT to mix the FANC PET and SPECT uniformity protocols providing that some SPECT specificities are taken into account.

KEY WORDS – SPECT, Uniformity, Quality control, Simulation, FANC

Introduction

The study investigated the possibility to mix for SPECT the FANC PET and SPECT transverse uniformity protocols [1,2] using standard reconstruction and processing tools widely available in a nuclear medicine department.

Materials and methods

Interactive Data Language (IDL) and GATE Monte Carlo (MC) simulations of SPECT were run for a cylinder filled with 740 MBq Tc99m radioactive water. Cylinder cavity was 280-mm tall and 180-mm in diameter and walls were 10 mm thick. The SPECT parameters were: cylinder centered in the field of view, 30-cm radius circular orbit, 360° rotation, 128 projections, 128*128 matrix (5.08 mm pixel), 10, 20 & 30 s projection times. IDL allowed to obtain noise free and Poisson noisy projections with and w/o attenuation but w/o spatial resolution simulation. An effective attenuation coefficient of 0.12 cm^{-1} was used to account for the scatter contribution. LEHR collimator and 140±14 keV energy window were used in MC to obtain noisy projections with attenuation, scattering and camera resolution effects. Thirty million counts flood uniformity images (5.08 mm pixel) were also generated with IDL and MC. Uniformity defects were generated by multiplying the projections or the flood images with a 2D Gaussian function of heights (H) from ±1.01 to ±1.20 and of three different FWHM (3, 6, 12 pixels). The Gaussian was centered at 9 locations in the same detector quadrant obtained by the combination of 3 radial (X) and 3 axial (Y) positions at 0, 51 and 76 mm from the cylinder center. Data were reconstructed with convolution ramp (cut-off at Nyquist) filtered backprojection. Attenuation was corrected using the first-order Chang method and an attenuation coefficient of 0.12 cm^{-1} (IDL) or 0.10 cm^{-1} (MC).

Reconstructed slices were processed as described in the FANC protocol [1]. The three most distal slices at each extremity of the phantom active volume were discarded and a centered circular ROI of 85% phantom inner diameter was drawn on each slice. Mean value (M) and standard deviation (SDM) as well as NEMA integral uniformity (IU) were computed in ROI.

The difference (DM) between M and the global mean of all processed slices were obtained. The standard deviation for DM (SDDM0) was obtained for the datasets without defect. DM and ± 2.5 SDDM0 were plotted against slice number. IU was computed for the flood images.

Results

Without defect, the noise (M/SDM) for the IDL or MC slices followed very closely the Jaszczak formula [2] and |DM| did not exceed 2.5 SDDM0.

Taking as criteria a single |DM| value higher than 3 SDDM0 or at least two |DM| values higher than 2.5 SDDM0, uniformity defects could be detected on IDL results for H ≤ 5% for all locations and FWHM but FWHM = 12 pixels, X = 76 mm and the three Y positions. In these three cases, a clear increase of IU was systematically observed for a lower H value than the H value where the above criteria was met by |DM| whereas it was the reverse for all other cases. IU seemed therefore to performed better than |DM| in some limit cases. H = 5% corresponded to flood IU lower than 3%. IDL data without attenuation but with noise allowed to show that the lowest H value to detect a defect with |DM| was 1-2% again at the exception of FWHM = 12 pixels and X = 76 mm for which H amounted to 5%.

For the MC data, DM plots were no more points randomly dispersed around a null value but a clear bended profile was observed as a result of the spatial resolution of the camera. A procedure involving a fit of this profile to the result of the convolution of a rectangle (geometric projection of the phantom physical inner volume) and a Gaussian that would take into account the camera resolution and possibly scatter will be presented as a potential solution to adopt the above criteria to these more realistic results.

Conclusion

The FANC procedure for PET transverse uniformity could be extended to SPECT and should allow the detection of defects corresponding to NEMA flood IU below 3% if SPECT limited spatial resolution and noise levels are accounted for and slice integral uniformity is in addition used.

References

[1] Federal Agency for Nuclear Control. [C - 2020/20334] Règlement technique fixant les critères d'acceptabilité pour les scanners PET (…) ainsi que les procédures concernées. *Belgisch Staatsblad/Moniteur Belge* 2020;03.03.2020:13087-13090.

[2] Federal Agency for Nuclear Control. [C - 2020/20339] Règlement technique fixant les critères d'acceptabilité pour les gamma-caméras (…) ainsi que les procédures concernées. *Belgisch Staatsblad/Moniteur Belge* 2020;03.03.2020:13100-13105.

[3] Jaszczak RJ, Coleman RE, Whitehead FR. Physical factors affecting quantitative measurements using camera-based SPECT. *IEEE TNS*. 1981;28:69-80. doi: 10.1109/TNS.1981.4331143.

Dosimetry Toolkit to determine radiation exposure in diagnostic Nuclear Medicine

Patrick Wanet, Virginie Kinnard, Anne-Sophie Hambye.
CHU Brugmann, Brussels.

ABSTRACT – We present a program allowing easy access to the most recently published data about recommended activities for various nuclear medicine examinations, as well as the related dosimetry.

KEY WORDS – Dosimetry, effective dose, diagnostic nuclear medicine, fetal exposure, recommended activity.

Introduction

We have developed a program to rapidly find the recommended activity and the related dosimetry for a large panel of diagnostic nuclear medicine examinations/radiopharmaceuticals. The program also provides links to all the published references on these subjects.

Materials and Methods

The program consists of 6 sections entitled Examination, Activity, Patient dosimetry, External doses, References and Guidelines. It also comprises links to various useful publications and websites. The first section includes data related to the patient (age, gestational status if applicable, weight) and to the examination/radiopharmaceutical. The second contains the optimal activity according to different sources (EANM, SNMMI, FANC). In the third section, the absorbed and effective doses are given, taking into account the data already introduced in the first section as well as the activity effectively administered. The fourth section adds additional information regarding the exposure in close contact and at 1 m from the full syringe. The last two sections provide a direct link to the references used to calculate the dosimetry and to the international guidelines.

In the first section, the type of examination/radiopharmaceutical must be selected from a list of approximately 90 possibilities. The patient's age category (adult, children 15, 10, 5 or 1 year old) has to be indicated, as well as the pregnancy status when applicable. Four possibilities are available depending on the gestation stage. The patient's weight is also requested to recommend the optimal activity that should be administered. All the dosimetric quantities come from data published in the literature and freely accessible via the Internet. The program has been written in HTML5/JavaScript.

Results

After completion of the first section, the recommended activity is calculated based on the EANM dosage card in children [1]. For adult patients, different activities are proposed, relying on the FANC DRL[2] values when available, on the EANM[3], and SNMMI guidelines[4]. Our own tables of standard activities are also given. SNMMI activities are

generally a little higher than EANM's. Our own tables are based on the lowest recommended activities in the international guidelines and are regularly updated.
In the third section, manual introduction of the actual administered activity is required. The absorbed dose is then given for the 3 most exposed organs/tissues, for the gonads and uterus and in some cases for the target organ (e.g., the brain for HMPAO). The values are expressed in µGy/MBq and calculated in mGy based on the administered activity chosen by the user. The effective dose for the patient is also indicated in µSv/MBq and calculated in mSv. In pregnant women, the program also shows the dose absorbed to the fetus, as well as, in appropriate cases (^{131}I and ^{123}I), the dose to the fetal thyroid. Section 4 reports the exposure in close contact to, and at 1 m from the syringe. In the Reference section, a simple click on hyperlinks will redirect the user to the dosimetric tables corresponding to the chosen radiopharmaceutical on the ICRP[5], or the RADAR[6] websites. The last section offers a direct link to the list of all guidelines from the EANM and SNMMI. For the completeness, a series of buttons provide direct access to various useful toolkits (SNMMI, EANM, RADAR). All the reported doses are based on ICRP publications, ICRP 128[7] in most cases, ICRP 80[8] or ICRP 53[9] for the others. For ICRP 53, the effective dose is given according to the old weighting factors. The corrected values can be found in a publication of the SFPM[10]. The doses to the fetus and to the fetal thyroid come from the publications of Russell (1999)[11], Stabin (2018)[12] and Watson (1992)[13] and those related to the syringe from the Delacroix report [14].

Conclusion

The aim of our program is to quickly find the most recent data published in the literature concerning the recommended activity to administer for various diagnostic procedures in nuclear medicine and the related radiation exposure. It can be easily used on any type of computers (Windows, Apple) as well as on any tablet or smartphone.

References

[1] European Association of Nuclear Medicine (EANM) https://www.eanm.org/content-eanm/uploads/2017/01/EANM_Dosage_Card_040214.pdf
[2] DRL (FANC) https://afcn.fgov.be/fr/professionnels/professions-medicales/medecine-nucleaire/obligations-reglementaires/nrd
[3] EANM Guidelines https://www.nucmed-guide.app/#!/startscreen
[4] Society of Nuclear Medicine & Molecular imaging (SNMMI) http://www.snmmi.org/ClinicalPractice/doseTool.aspx?ItemNumber=11216&navItemNumber=11218
[5] International Commission on Radiological Protection (ICRP) https://www.icrp.org/page.asp?id=5
[6] RADAR Report Michael G. Stabin, Jeffry A. Siegel. http://www.doseinfo-radar.com/Adult-peds.docx
[7] ICRP 128(2015) https://journals.sagepub.com/doi/pdf/10.1177/ANIB_44_2S
[8] ICRP 80 (1998) https://journals.sagepub.com/doi/pdf/10.1177/ANIB_28_3
[9] ICRP 53 (1987) https://journals.sagepub.com/doi/pdf/10.1177/ANIB_18_1-4
[10] Société Française de Physique Médicale. Report SFPM 19-2001. https://inis.iaea.org/collection/NCLCollectionStore/_Public/43/054/43054871.pdf.
[11] J. Russell, M. Stabin, R. Sparks, E. Watson. Radiation Absorbed Dose to the Embryo/Fetus from Radiopharmaceuticals http://www.doseinfo-radar.com/pregtables.doc
[12] New Generation Fetal Dose Estimates for Radiopharmaceuticals. Michael G. Stabin https://jnm.snmjournals.org/content/jnumed/early/2017/12/20/jnumed.117.204214.full.pdf
[13] E. Watson. Radiation Absorbed Dose to the Human Fetal Thyroid https://www.doseinfo-radar.com/RADAR-INT-NM.html
[14] D. Delacroix et al. http://www.hep.ucl.ac.uk/~saakyan/phas0052/Radionuclide_Data_Handbook.pdf